

Influence of thickness on the structural, optical and electrical properties of CuInSe_2 absorbing layer for photovoltaic applications

XIN JI*, YIMING MI, ZHI YAN^a, CHAO MIN ZHANG

College of Fundamental Studies, Shanghai University of Engineering Science, Shanghai 201620, China

^aCollege of Material Engineering, Shanghai University of Engineering Science, Shanghai 201620, China

Solar cell absorbing layer based on CuInSe_2 films were successfully deposited by magnetron RF-sputtering with different film thicknesses (300, 450, 600, 750 and 1100 nm). The effect of film thickness on the film structures, morphologies and properties was investigated in detail. The results show that the increase of film thickness is in favor to be constituted in a chalcopyrite structure with a preferential orientation of (112), (220) and (204) diffraction planes. The morphologies results implied the films become rougher and the grain size increase when film thickness increased from 300 nm to 1100 nm. Furthermore, it is indicated that 1100 nm is the best film thickness in electrical and optical properties in the all samples.

(Received January 19, 2012; accepted April 11, 2012)

Keywords: Thin film, CuInSe_2 , Film thickness, Vapor deposition, Optical properties

For several years the study of ternary compounds has been intensified in order to find new materials for solar photocells [1, 2]. The development of thin film solar cells is an active area of research at this time. Recently, much attention has been paid to the development of low cost, high efficiency thin film solar cells [3]. Among the I-III-IV₂ compounds, CuInSe_2 is one of the suitable candidates for the production of thin film solar cells due to its ideal band gap, high absorption coefficient and ease of film fabrication. $\text{CuInSe}_2/\text{CdS}$ solar cells are one of the prospective candidates for widespread commercial success in solar energy conversion [4]. They can be produced at low price with good efficiency and excellent stability.

Various techniques such as RF-magnetron sputtering [5], co-sputtering [6], flash evaporation [7], chemical spray [8] and electro-deposition [9] have been investigated as suitable techniques for the fabrication of CuInSe_2 thin films. Enormous amount of work has been already reported on structure, optical and electrical properties of CuInSe_2 thin films [10, 11]. However, still it requires further investigation to optimize the optical and electrical properties of CuInSe_2 films to use as a suitable candidate for solar cell applications.

It is well known that properties of CuInSe_2 films are strongly dependent on the preparation methods and deposition parameters [12, 13] due to obtained stoichiometry and microstructure. For this reason, it is essential to characterize their properties according to the deposition parameters.

In this paper, we report the preparation of high-quality CIS nanocrystalline thin films on SFO glass substrates, using a RF-magnetron sputtering technique. The effect of the film thickness of nanocrystalline CIS films on the electro-optical performance of solar cells was investigated.

1. Experiment

1.1 Synthesis of CuInSe_2 thin films

Thin films of CIS were deposited by RF-sputtering in argon gas atmosphere on SFO (SnO_2 : F) glass substrates. Substrates were cleaned ultrasonically and chemically in organic solvents. A CdS film layer was deposited firstly on the SFO glasses using a power of 50 W, and then the CuInSe_2 absorbing layer was deposited. A cylindrical CIS (Cu: In: Se = 1: 1: 2) single ceramic target of 60 mm diameter was used. No changes in target composition were observed with time. All films were deposited at the substrate temperature 200 °C, at a working gas pressure of 0.5 Pa and a sputtering power of 100 W. The samples were deposited at the different sputtering times (1.0, 2.0, 2.5, 3.0 and 4.0 h). The process parameters of CIS films used in RF magnetron sputtering are shown in Table 1.

Table 1. Sputtering parameters of CuInSe_2 films.

Sample	Sputtering time / (h)	Sputtering power / (W)	Sputtering temperature / (°C)
a	1.0	100	200
b	2.0	100	200
c	2.5	100	200
d	3.0	100	200
e	4.0	100	200

1.2 Characterizations of CuInSe_2 films

Optical properties were determined from measurements

of optical transmittance at room temperature with unpolarized light at normal incidence in the photon energy range of 1.1-6.6eV. The resistivity calculated from the sheet resistance measured by a four-point probe. Coupled θ -2 θ X-ray diffraction (XRD) scans in the film mode were performed in the range of $2\theta=20^{\circ}$ - 80° by using of the Cu K α 1 line of the X-ray source (Rigaku D/max2550) to investigate crystallographic properties of the films. The surface morphologies of films were examined by scanning electron microscopy (SEM-3400-N) and atomic force microscopy (DI Nano-scope IIIA Multimode). The AFM image analysis was carried out using commercial WSxM 4.0 (Nanotec Electronica) software procedures to determine the surface roughness characterized by the Root-Mean-Square (RMS) parameter.

2. Results and discussion

2.1 Structural studies of CuInSe₂ films

The Cu K α X-ray diffraction patterns of the CuInSe₂ films prepared with different thicknesses (300, 450, 600, 750 and 1100nm) are shown in Fig.1. The chalcopyrite structure is mainly confirmed by the (1 1 2), (2 2 0) and (2 0 4) diffraction peaks at $2\theta = 26.7^{\circ}$, 34.2° and 44.6° , which followed by a tetragonal structure confirmed by (3 1 0) and (3 1 2) peaks at $2\theta = 51.8^{\circ}$, 54.6° [13]. By film thicknesses increased, CuInSe₂ films exhibit not only stronger diffractions but also (1 1 2), (2 1 1) and (3 1 0) preferred-orientation, indicating that CuInSe₂ films with high crystalline are easier to grow in the thicker films. Moreover, the width of half peak always represents the larger grain size, strain and dislocation density on film thickness [14, 15].

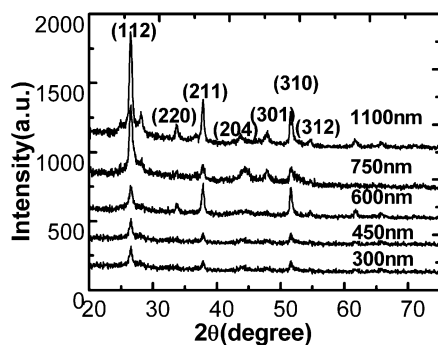


Fig. 1. XRD patterns of CuInSe₂ films deposited at different thicknesses

2.2 Morphological studies of CuInSe₂ films

The CuInSe₂ films have been analyzed by SEM techniques in order to observe and study the surface morphologies and the film thicknesses. Thicknesses of the film measured as a function of sputtering times are shown in Fig. 2.

Obviously, it can be found in Fig. 2 that the film became much thicker with increase of sputtering times, which led to the improvement of the crystallinity [16]. It has been observed that thinner films were deposited at longer sputtering times (>2.5 h) while thicker non-adherent films were formed for the shorter sputtering times (<2.0 h) [17].

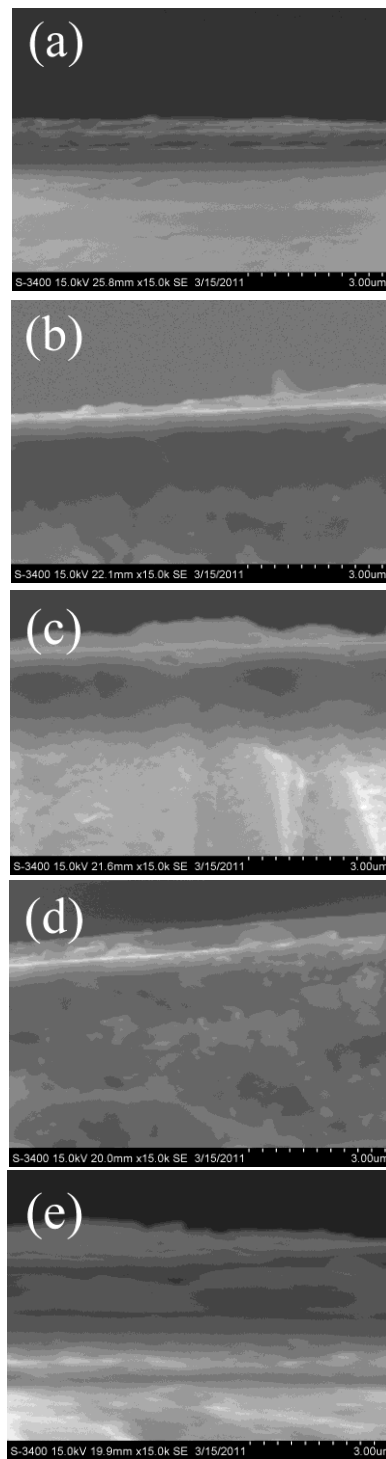


Fig. 2. SEM images of cross sections in CuInSe₂ films deposited with different film thicknesses: (a) 1.0 h, (b) 2.0 h, (c) 2.5 h, (d) 3.0 h and (e) 4.0 h.

Fig.3 shows that the films deposited at 300nm have a few isolated grains (CuInSe₂ grains) with uniform size and well-defined boundaries on the SFO substrates at low sputtering rate. When the film thickness of 450nm deposited, the grain boundaries become irregular and some of the grains are connected due to the increase of the solute concentration or variation of the applied potentials [18]. However, the shapes of grains were changed from the circular to the strip when the thickness increased from 450 to 600nm. Also, expand of surface defect density as the increase of the thickness can be seen in Fig.3.

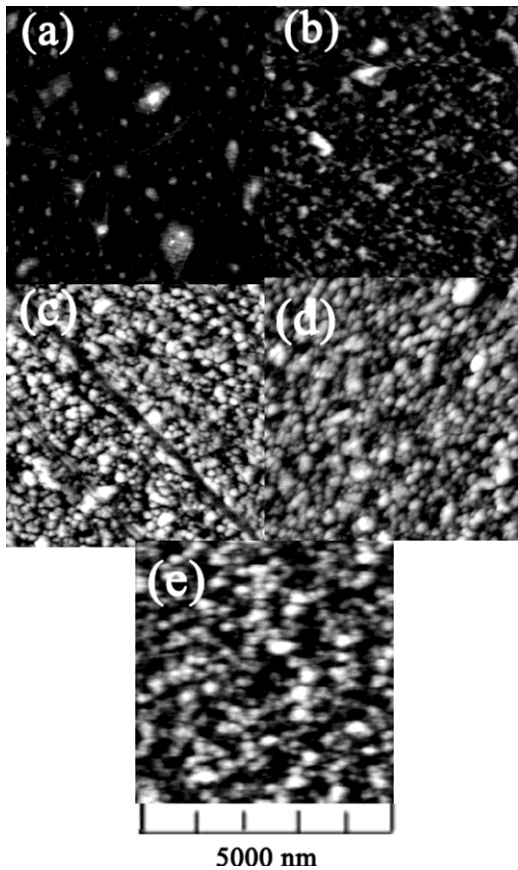


Fig. 3. AFM images of surface morphologies in CuInSe₂ films deposited for different thickness: (a) 300 nm, (b) 450 nm, (c) 600 nm, (d) 750 nm, (e) 1100 nm.

Tab.2 summarizes the data of grain size and film thickness resulted from Fig. 2 and Fig. 3. It can be seen from Tab.2 that the films became rougher when film thickness increased from 300nm to 1100nm. Additionally, a comparison between the micrograph (e) and the previous micrographs (a-d) revealed clearly a significant increase in the average grain size of the film (1100nm) and apparition of pinholes as well [19].

Table 2. Variation of grain diameters and surface roughness of CIS films prepared at different film thickness.

Sample	Sputtering times / (h)	Film thickness / (nm)	Grain diameter / (nm)	Surface Roughness / (nm)
a	1.0	300	36.26	1.37
b	2.0	450	43.62	6.76
c	2.5	600	88.35	10.55
d	3.0	750	96.20	15.32
e	4.0	1100	112.59	18.35

2.3 Electrical properties of CuInSe₂ films

Fig. 4 illustrates the resistivity calculated from the sheet resistance measured by a four-point probe as a function of the film thickness for CIS films. It is observed from Fig. 4 that the electric conduction of CIS films decrease gradually with film thickness. Obviously, the CIS films deposited at 1100nm shows better electrical behavior than other films. The plot also reveals that the resistance of the films depends strongly on the film thickness. It is due to the presence of large grains with more copper deficiencies in the thicker films [20]. Moreover, Surface roughness and grain size of films have direct correlation with the electrical properties. In general, as the film thickness increases, the grain size and the surface roughness increase which results in the increase in surface defect density [21] which can reduce carrier lifetime. Also, the number of interface states between the CIS films and the substrates always are cut down due to their smooth surfaces [22].

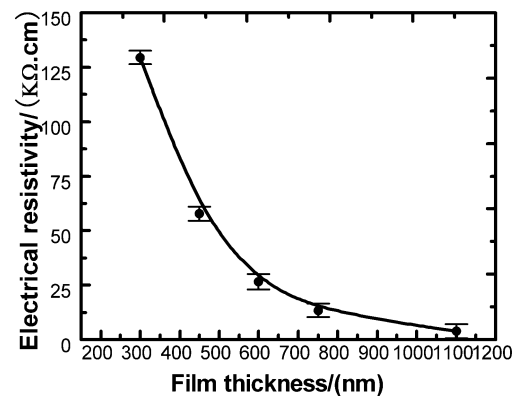


Fig. 4. The resistivity of CuInSe₂ films deposited for different thicknesses.

2.4 Optical properties of CuInSe₂ films

Fig. 5 shows the transmittance spectra of CIS films deposited for different film thickness in the wavelength range 200-1100nm. It can be observed that a slight increase in the absorption in the IR region with the increase of the film thickness. This behavior was consistent with the increase of

the grain sizes after the thicker film deposited [23]. Moreover, it also can be found that the transmission in the visible region increased obviously with the decrease of film thickness. The optical transmission of the CIS films in 1100nm was lower than the other films in the wavelength region above 800 nm. This is attributed to the increase in free-carrier absorption due to the low electron mobility of the films [24].

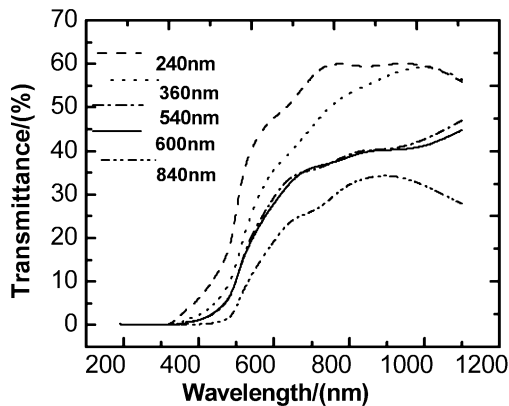


Fig. 5. Transmittance spectra curves of CuInSe_2 films deposited for different thickness.

3. Conclusions

Thin films of CuInSe_2 have been grown on SFO (SnO_2 : F) glass substrates with different film thicknesses. The XRD patterns reveal that the CuInSe_2 films with high crystallinity are easier to grow in the thicker films. Moreover, the width of half peak always represents the larger grain size, strain and dislocation density on film thickness. In addition, it is also observed that the resistance of the thicker film is found to be comparatively less than that of thinner films. The optical measurements suggest that not only grain sizes but also film thickness affected the optical properties of the films.

Acknowledgements

This work is supported by the Shanghai Municipal Education Commission's Fund for the Outstanding Young Teachers in High Education Institutions (No: shgcjs021) and the Academic Program of Shanghai Municipal Education Commissions (grant nos 11XK11 and 2011X34).

References

- [1] X. Ji, Y. M. Mi, Z. Yan, C. M. Zhang, *Optoelectron. Adv. Mater. – Rapid Commun.* **5**(9), 977 (2011).
- [2] M. A. Popescu, J. Non. – *Cryst. Solids.* **169**(1-2), 155 (1994).
- [3] X. Ji, Z. Yan, Y. M. Mi, C. M. Zhang, *Optoelectron. Adv. Mater. – Rapid Commun.* **6**(1-2), 300 (2012).
- [4] M. A. Popescu, J. Non-Cryst. Solids. **35-36**, 549 (1980).
- [5] N. Djedid, B. Hadoudja, B. Chouial, S. Yousfi, A. Chibani, *Optoelectron. Adv. Mater.–Rapid Commun.* **5**(8), 827 (2011).
- [6] M. Chandramohan, T. Venkatachalam, *Optoelectron. Adv. Mater. –Rapid Commun.* **4**(1), 70 (2010).
- [7] M. Venkatachalam, M. D. Kannan, S. Jayakumar, R. Balasundaraprabhu, N Muthukumarasamy, *Thin Solid Films.* **20**, 516 (2008).
- [8] F. Chowdhury, J. Begum, M. S. Alam, S. M. F. Hasan, *Optoelectron. Adv. Mater.-Rapid Commun.* **4**(12), 2039 (2010).
- [9] Z. Rizwan, B. Z. Azmi, M. G. M. Sabri, *Optoelectron. Adv. Mater. – Rapid Commun.* **5**(4), 393 (2011).
- [10] F. Yakuphanoglu, W. A. Farooq, *Optoelectron. Adv. Mater. – Rapid Commun.* **5**(2), 153 (2011)
- [11] Z. Rizwan, N, B. Z. Azmi, M. G. M. Sabri, *Optoelectron. Adv. Mater. –Rapid Commun.* **5**(4), 393 (2011).
- [12] V. Senthamilselvi, K. Saranakumar, R. Anandhi, A. T. Ravichandran, K. Ravichandran., *Optoelectron. Adv. Mater. –Rapid Commun.* **5**(10), 1072 (2011).
- [13] T. C. Sadler, M. J. Kappers, R. A. Oliver, J. Cryst. Growth. **311**, 3380 (2009).
- [14] K. Senthil, D. Nataraj, K. Prabakar, D. Mangalaraj, S. K. Narayandass, N. Udhayakumar, N. Krishna kumar. *Mater Chem Phys.* **58**, 221 (1999).
- [15] M. Dhanam, R. Balasundaraprabhu, S. Jayakumar, S. Gopalakrishnan, M. D. Kannan, *Phys Stat Sol A.* **191**, 149 (2002).
- [16] F. Kang, J. P. Ao, G. Z. Sun, Q. He, Y. Sun. *J. Alloys Compd.* **478**, L25 (2009).
- [17] P. P. Hankare, K. C. Rathod, P. A. Chate, A. V. Jadhav, I. S. Mulla, *J. Alloys Compd.* **500**, 78 (2010).
- [18] L. Zhang, F. D. Jiang, J. Y. Feng. *Solar Energy Mater. Sol. Cells.* **80**, 483 (2003).
- [19] A. Gobeaut, L. Laffont, J. M. Tarascon, L. Parissi, O. Kerrec. *Thin Solid Films.* **517**, 4436 (2009).
- [20] L. Djellal, S. Omeiri, A. Bouguelia, M. Trari. *J. Alloys Compd.* **476**, 584 (2009).
- [21] B. Canava, J. Vigneron, A. Etcheberry, J. F. Guillemoles, D. Lincot, *Appl. Surf. Sci.* **202**, 8 (2002).
- [22] A. M. Hermann, M. Mansour, V. Badri, B. Pinkhasov, C. Gonzales, F. Fickett, M. E. Calixto, P. J. Sebastian, C. H. Marshall, T. J. Gillespie. *Thin Solid Films.* **74**, 361 (2000).
- [23] I. Dirnstorfer, W. Burkhardt, W. Kriegseis, I. Osterreicher, H. Alves, D. M. Hoffman, O. Ka, A. Polity, B. K. Meyer, D. Braunger. *Thin Solid B. Films.* **361/362**, 400 (2000).
- [24] S. Zhang, D. Sun, Y. Fu, H. Du, Q. Zhang, *Diamond Relat. Mater.* **13**, 1777 (2004).

*Corresponding author: jixinyouxiang1@yahoo.com.cn